



## RESEARCH LETTER

10.1002/2016GL072097

## Key Points:

- Tropical expansion is largely attributed to natural variability
- CMIP5 climate models can reproduce part of this tropical expansion without any type of forcing
- This tropical expansion is largely forced by SSTs in the Tropical Pacific with SSTs in the Indian Ocean playing a secondary role

## Supporting Information:

- Supporting Information S1

## Correspondence to:

D. F. Mantsis,  
d.mantsis@unsw.edu.au

## Citation:

Mantsis, D. F., S. Sherwood, R. Allen, and L. Shi (2017), Natural variations of tropical width and recent trends, *Geophys. Res. Lett.*, 44, 3825–3832, doi:10.1002/2016GL072097.

Received 1 DEC 2016

Accepted 28 FEB 2017

Accepted article online 6 MAR 2017

Published online 24 APR 2017

## Natural variations of tropical width and recent trends

Damianos F. Mantsis<sup>1</sup> , Steven Sherwood<sup>1</sup> , Robert Allen<sup>2</sup> , and Lei Shi<sup>3</sup> 

<sup>1</sup>Climate Change Research Centre, University of New South Wales, Sydney, New South Wales, Australia, <sup>2</sup>Department of Earth Sciences, University of California, Riverside, California, USA, <sup>3</sup>National Centers for Environmental Information, NOAA, Ashville, North Carolina, USA

**Abstract** The temporal evolution of the tropical width since 1979 is investigated in observations and models by using metrics based on outgoing radiation, 6.7  $\mu\text{m}$  brightness temperature, and atmospheric reanalysis. The maximum 20 year widening as seen in radiation by satellites occurred during 1993–2012 and was associated with a global sea surface temperature (SST) change that resembles the El Niño–Southern Oscillation/Pacific Decadal Oscillation in the Pacific region. Idealized experiments with Community Atmospheric Model version 5 reveal that Tropical Pacific SST pattern largely accounts for the widening. A number of Coupled Model Intercomparison Project Phase 5 coupled models can simulate, without any type of forcing, this satellite-inferred tropical widening and its associated Pacific SST pattern. While model-simulated widenings are consistent for all metrics, the two reanalysis-based widenings are inconsistent internally and with the satellite-based and model widenings. Our results reinforce suggestions that observed widenings can be explained by internal variability as captured by climate models, though this depends on whether reanalysis trends are regarded as reliable.

## 1. Introduction

Observations suggest that the subtropics have shifted toward the poles by several degrees between the late 1970s and early 2000s [Hu and Fu, 2007; Seidel et al., 2008; Lucas et al., 2014]. This can be seen in a variety of observational approaches, suggesting that this is a robust finding [Davis and Rosenlof, 2012], although studies differ on the rate of expansion [Quan et al., 2014]. This topic has drawn much attention due to the potential implications of such circulation shifts for future rainfall in subtropical and midlatitude regions.

A number of possible causes have been identified. Idealized and more realistic climate studies indicate that warming induced by greenhouse gas (GHG) emissions will result in an increase in the subtropical static stability, pushing the baroclinic instability zone and the Hadley cell edge poleward [Lu et al., 2007]. However, the simulated trend is considerably smaller than observed [Johanson and Fu, 2009; Nguyen et al., 2015]. Expansion in the Southern Hemisphere has also been attributed to stratospheric cooling as a result of ozone depletion over Antarctica [Son et al., 2009; Son et al., 2010; Polvani et al., 2011; McLandress et al., 2011; Kang et al., 2012; Allen et al., 2012; Hu et al., 2013; Waugh et al., 2015] and GHGs [Nguyen et al., 2015]. In contrast, the expansion in the Northern Hemisphere has been hypothesized to be driven by anthropogenic emissions of black carbon and tropospheric ozone [Allen et al., 2012; Kovilakam and Mahajan, 2015].

Regarding the ability of sea surface temperature (SST) changes to account for tropical widening, previous studies are inconclusive. Some find that Coupled Model Intercomparison Project Phase 3 (CMIP3) simulations forced with observed SST changes cannot reproduce the observed tropical expansion [Lu et al., 2009], although some of these lacked black carbon and tropospheric ozone emissions, which appear to bring simulations closer to observations [Allen et al., 2012].

Meanwhile, on decadal time scales, tropical width variations over Asia derived from tropospheric height-based metrics have been shown to be associated with those of central North Pacific SSTs, accounting for roughly 50% of the expansion trend [Lucas and Nguyen, 2015], suggesting a role for natural variability, in particular the Pacific Decadal Oscillation (PDO). The significance of such an association is impossible to gauge from observations alone, however, since tropical width has been observed only for roughly one PDO cycle. Grassi et al. [2012] has also pointed out that a switch of the PDO from a positive to a negative phase can lead to a widening of the tropical belt during the equinoxes. However, experiments with an older version of the Community Atmospheric Model (CAM3.5) forced with a PDO SST were noticed to underestimate the observed widening, due to an incorrect model-simulated convective response to tropical SSTs. In contrast,

experiments with a newer version of the Community Atmospheric Model (CAM5) forced with observed SSTs showed seasonal patterns of expansion in a slightly better agreement with observations, albeit still significantly underestimating overall trends [Allen *et al.*, 2014].

The focus of this study is to show that CMIP5 coupled models are able to simulate a significant portion of the observed tropical expansion and that this is associated with an SST pattern that resembles the PDO/El Niño–Southern Oscillation (ENSO).

## 2. Data and Methods

Our analysis makes use of a range of satellite data. We use outgoing longwave radiation (OLR) from both the advanced very high resolution radiometer (AVHRR, 1979–2013) and the High-Resolution Infrared Radiation Sounder instrument (1979–2015), as well as a homogenized record of brightness temperature (BT) from the HIRS channel 12 (centered at 6.7  $\mu\text{m}$ ), which observes the upper tropospheric humidity (1979–2014). These are described in more detail in the supporting information.

All records of tropical width contain potential bias changes over time. It has been noted that the OLR (AVHRR) record may contain artificial trends associated with changes in the equatorial crossing time or instrument calibration, which could affect inferred tropical width changes [Lucas *et al.*, 2014]. One reason to include the HIRS OLR here is that an attempt has been made to remove these effects from this record. Another problem with broadband OLR is that it not only reflects temperature at the surface, the troposphere, and stratosphere but also changes in water vapor, clouds, and aerosols, each one affecting a different portion of the spectrum, and so does not have a simple physical interpretation [Lucas *et al.*, 2014]. That is why we include HIRS BT in our analysis, since it measures relative humidity in the upper-middle troposphere (200–600 hPa) which is closely linked to the overturning circulation [e.g., Sherwood, 1996]. Also, HIRS channel 12 only measures between clouds. This means that long-term changes in the water vapor content of the lower-to-middle troposphere or clouds are not accounted for. Note though, that HIRS BT can be affected by aerosols from major volcanic eruptions. Despite the fact that several issues have been noted with satellite-derived OLR products (more details in section 4), these have the advantage of being the only purely observational record with reliable coverage in space and time.

In order to estimate the position of the subtropical edge based on OLR, we avoid the traditional definition based on an absolute threshold because it can result in spurious trends due to global temperature or instrument bias changes [Davis and Rosenlof, 2012]. Instead, we use relative thresholds, estimated as the latitude where the zonal mean OLR drops 20  $\text{W m}^{-2}$  on the poleward side of the position of its subtropical maximum, following Davis and Rosenlof [2012]. The same methodology is used for brightness temperature, except that the subtropics are estimated where the zonal mean drops by 2 K on the poleward side of the zonal mean maximum, which is located around 20° latitude (Figure S1 in the supporting information).

We also consider two additional metrics to define the subtropical edge: (1) where the zonal mean meridional streamfunction (MMC) becomes zero at 500 hPa on the poleward side of the subtropical maximum and (2) where the zonal mean precipitation minus evaporation becomes zero ( $P-E=0$ ) on the poleward side of the subtropical minimum. However, we will argue that observational estimates of these measures, which must be obtained from reanalysis data, are less stable over time than those from satellites.

In order to investigate whether the tropical expansion seen in observations can be explained by natural variability, we use unforced simulations of 14 coupled models from the CMIP5 archive (Table S1 in the supporting information). Using CAM5, the atmospheric component of the Community Earth System Model version 1.2, we investigate the relationship between the SST forcing and the expansion of the tropical belt.

## 3. Results

### 3.1. Satellite Observations and Reanalysis

All three satellite products show that since 1979, the tropics have become considerably wider, mostly due to a poleward shift in the subtropics in the Northern Hemisphere. This widening is 0.45°, 0.21°, 0.65°/decade for AVHRR-OLR, HIRS-OLR, and HIRS-BTEMP, respectively (Figure 1). However, this widening is not separated equally in the two hemispheres and among data sets and the agreement between the three satellite products is less obvious when the evolution of the position of the subtropics is examined in the two hemispheres

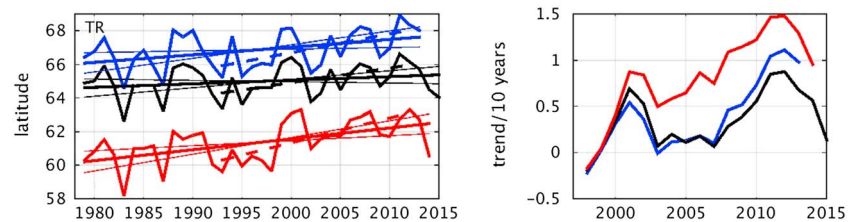


**Figure 1.** (right) Evolution of tropical width. The dashed lines represent the 1993–2012 trend. The solid bold lines represent the overall trend, and the solid thin lines represent the trend with the slope replaced by the values corresponding to the 95% confidence interval. (left) Evolution of the 20 year trends of tropical width (each point represents the end year of the 20 year period). The blue, black, and red colors represent OLR-AVHRR, OLR-HIRS, and brightness temperature, respectively.

separately (Figure S2). For the NH, all three products show that the subtropics are expanding,  $0.61^\circ$  for AVHRR OLR,  $0.18^\circ$  for HIRS OLR, and  $0.49^\circ/\text{decade}$  for HIRS brightness temperature. On the other hand, in the SH, some disagreement among the data sets exists. HIRS OLR and brightness temperature show an expansion by  $-0.03^\circ$  and  $-0.16^\circ/\text{decades}$ , respectively, but AVHRR OLR shows a contraction by  $0.16^\circ/\text{decade}$ .

It has been previously noted that trends in the tropical width may be excessively large in the AVHRR OLR due to artificial biases [Lucas *et al.*, 2014], and therefore, the trends seen in the HIRS OLR might be more realistic since such biases have been accounted for. Also, the larger trend exhibited by BT, compared to OLR, might be due to the fact that it reflects changes in the upper-middle tropospheric humidity only. By definition, BT does not account for the effect from clouds, anthropogenic aerosols, or water vapor from middle lower troposphere, which might reflect a different expansion rate. Note, however, that the BT can be affected by large volcanic eruptions, as seen by the contraction of the tropical belt after the eruption of Mt Pinatubo in 1991. Nevertheless, similar patterns of BT in the changes of the subtropical evolution rates further support the conclusion derived from OLR data sets.

This widening since 1979, however, has not been constant. Moving 20 year trends (Figure 1) show that the widening was strongest during roughly 1993–2012, with a secondary peak during the period of 1982–2001, according to all three satellite products, which show a striking qualitative agreement. This implies that the tropical widening observed during the last 36 years is significantly affected by natural variability on decadal time scales. Indeed, the widening during 1993–2012 ( $1.6\text{--}3^\circ$ ) more than accounts for all of that during the overall (1979–2015) record ( $0.8\text{--}2.3^\circ$ ), and the rapid reduction of the 20 year trend over the last few years further supports this claim.

We applied the same analysis to the MMC metric in four reanalysis products (R1, R2, ERA-Interim, and Japanese 55-year Reanalysis), which yielded a much wider spread in widening rates, ranging from  $0.56^\circ$  to  $1.37^\circ/\text{decade}$  on the overall trend and  $0.9^\circ$  to  $2.7^\circ/\text{decade}$  for the peak 20 year trend depending on reanalysis. A similar spread is exhibited by reanalysis P-E trends [Davis and Rosenlof, 2012, Figure 2]. The large absolute magnitude of these ranges shows that 20 year trends cannot be estimated accurately; they will be affected by inhomogeneities in reanalysis data [e.g., Hartman *et al.*, 2013], especially since neither metric is directly constrained by observations going into the reanalyses.

The pattern of OLR (Figure 2) trend for 1993–2012 (i.e., at each grid point, we plot the slope of the 20 year trend for OLR) consists of an increase over the equatorial West Pacific extending toward the Southeast Pacific. To the west, an anomaly of the opposite sign takes place, enclosing the positive anomaly in a horse-shoe pattern. During the same period, Pacific SST trends exhibit a pattern (i.e., the slope of the 20 year trend for SST is plotted at each grid point) with a strong north-south symmetry, resembling the PDO [Newman *et al.*, 2016], which involves a broad cooling of the Tropical Central-East Pacific and a small warming to the west, strengthening the west-east SST gradient. In contrast, at higher latitudes in both hemispheres, the SST anomalies exhibit a wider warming in the west-central basin and a much narrower cooling in the east close to the coast of the Americas. Regarding the other basins, such an asymmetry is not present, but the simultaneous warming in the north Atlantic and Indian Ocean gives a symmetric component in the zonal mean sense and model experiments will show whether this has an additional effect on the width of the tropics. During the period of 1982–2001 where the tropical width experiences a secondary peak, the OLR and SST trend pattern exhibit strong similarities with those of the period 1993–2012 (not shown), suggesting that the tropical width is regulated by the same physical mechanism.

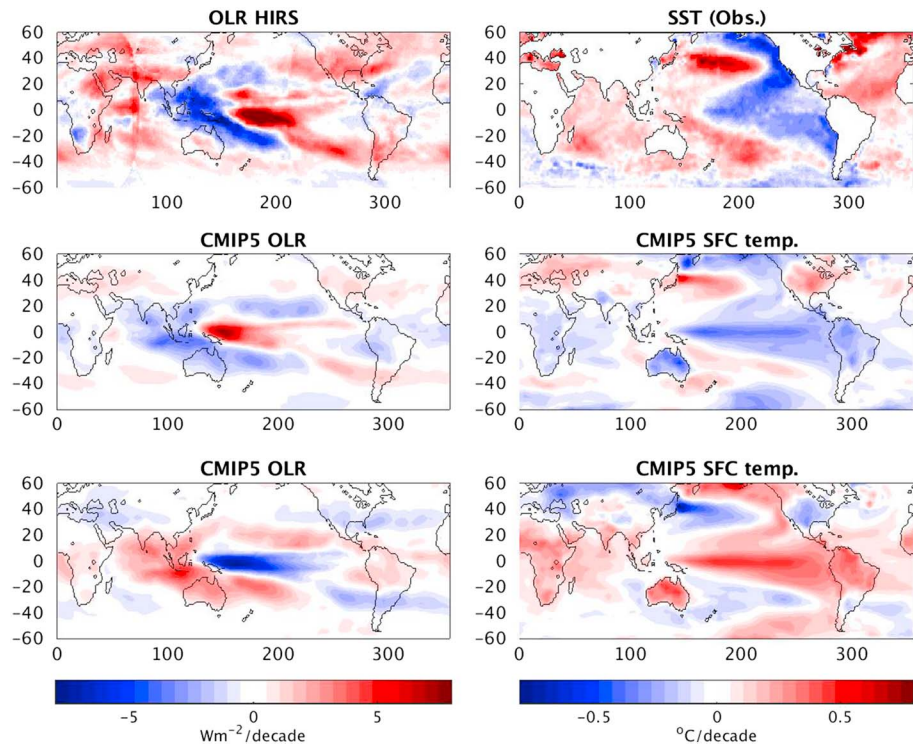


**Figure 2.** (top) OLR and SST/surface (SFC) temperature trend for the period of 1993–2012 from observations. Ensemble mean (14 CMIP5 models) trend for annual OLR and SFC temperature that corresponds to the 20 year period where the tropical width experiences (middle) Max (expanding) trends and the (bottom) Min (contracting) trends.

**3.2. CMIP5 Models**

An examination of unforced (control) simulations with 14 coupled models from the CMIP5 archive (Table S1), of duration of several hundred years, shows that the width of the simulated tropics, estimated based on OLR, can experience a maximum 20 year trend (contraction or expansion) that is comparable or even bigger than

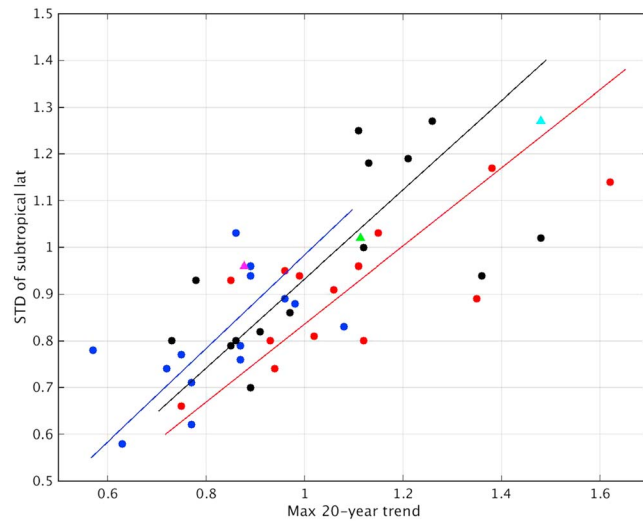


**Figure 3.** Scatterplot of maximum 20 year trend versus the interannual variability in tropical width. The blue markers correspond to MMC, the red correspond to P-E, and the black correspond to OLR. The circles correspond to individual models, and the triangles correspond to the 1993–2012 trend from satellite observations: AVHRR OLR (green), HIRS OLR (purple), and HIRS brightness temperature (cyan).

those observed (Figure 3). Ten models exhibit stronger maximum trends compared to the ones observed in the HIRS OLR and seven do so for AVHRR OLR. Comparable expansion rates are given by P-E and MMC. The ensemble means from OLR, P-E, and MMC are 1.09°, 1.05°, and 0.83° decade<sup>-1</sup>, respectively. This highlights the fact that the magnitude of the expansion/contraction in the unforced CMIP5 simulations is rather independent on the metric used to define the width of the tropical belt. It should be noted that for each CTRL, the maximum 20 year trend does not take place during the same time, when the width of the tropics is estimated from the three different metrics. Despite this, for every model, the year-to-year variations of the three width metrics correlate positively with each other at 99% significance level,



with average correlations ranging from 0.58 (for correlation between OLR and P-E) to 0.7 (for correlation of MMC with OLR and P-E).

Also, among models, the highest 20 year trend in each metric roughly scales with the interannual variability of the metric in the same model (Figure 3). Comparing the two hemispheres gives a similar result, and for each metric, the hemisphere that experiences larger interannual variability experiences a proportionately larger maximum trend (i.e., for P-E, both are 80% stronger in the NH; for MMC, both are 30% stronger; for OLR, both are 10% weaker compared to the SH). Also, models that experience large 20 year expanding trends also experience 20 year contracting trends of comparable magnitude, which supports the notion that interannual variability determines, to a great extent, the ability of models to simulate the observed tropical expansion rate.

Figure 2 shows the ensemble mean OLR trend pattern during the period of most rapid 20 year expansion in the CMIP5 control runs. Reasonable agreement between models and observations is found, especially over the Pacific, despite the fact that models position the maximum OLR trend anomaly slightly to the west compared to observations, and with a slightly smaller magnitude. On the other hand, models and observations disagree over the Indian Ocean; i.e., the simulated trends over Indonesia extend too far to the west over the Indian Ocean, unlike observations where the trends switch sign. Furthermore, the corresponding SST trends (Figure 2) similarly resemble the observed SST trends, in spite of some differences. For example, the cooling in the Tropical Pacific extends too far to the west (like OLR); over the Indian Ocean, the trends have the opposite sign; and the midlatitude warming is slightly underestimated, especially in the Southern Pacific. CMIP5 coupled models also give us the ability to estimate the OLR and SST patterns associated to the maximum contraction, which are similar with those corresponding to the maximum expansion, but with the opposite sign.

But is this SST trend pattern uniquely associated with maximum tropical expansion (or contraction) based only on one metric (OLR in this case)? For this we re-estimated the SST trend pattern during periods of maximum expansion according to the other two metrics, i.e., P-E and MMC (Figure S3). All three metrics produce fairly similar patterns. This implies that the simulated tropics will acquire its maximum width through a similar mechanism (similar SST pattern) regardless of the metric used to estimate the width.

However, what is the source of this natural climate variability? Large volcanic eruptions have been shown to induce a short-term contraction in the tropics, especially when using tropopause height-based metrics, by warming the lower stratosphere and lowering tropopause height [Lucas *et al.*, 2012, 2014]. Additionally, it has been argued that volcanic eruptions of global significance might trigger El Niño events or even augment pre-existing ones [Emile-Geay *et al.*, 2007]. This means that the El Chichon (1982) and Mt. Pinatubo (1991) eruptions might have affected the variability of the tropical width on the short time scales used in this study. ENSO events have also been previously suggested to affect the tropical edge at interannual time scales [Lu *et al.*, 2008; Adam *et al.*, 2014; Lucas and Nguyen, 2015], which implies that its effect could show up as a residual over decadal time scales.

### 3.3. CAM5 Idealized Experiments

The SST-forced idealized experiments with CAM5 are run at  $1.9^\circ \times 2.5^\circ$  horizontal resolution. First we conduct a 45 year long control run (CTRL) where the model is forced with the 1982–2001 climatological SSTs (seasonal SST cycle) repeated over 45 cycles. We also run additional simulations where the SST forcing consists of the climatological cycle plus the 1993–2012 linear trend. The first experiment includes the trend from  $65^\circ\text{S}$  to  $65^\circ\text{N}$  (called GLOB). We also conduct four additional experiments where the SST trend included in GLOB is used but only from a certain oceanic region: (a) Atlantic Ocean, (b) Indian Ocean, (c) Tropical Pacific from  $25^\circ\text{S}$  to  $25^\circ\text{N}$ , and (d) High-latitude Pacific Ocean from  $25^\circ$  to  $65^\circ$  degrees in both hemispheres. All runs are 45 years long. To diagnose the contribution of the SST trend from each basin to the tropical expansion, we compare the subtropical edge from CTRL to all the other experiments.

Our experiments show that the SST trend does result in a widening of the tropics regardless of the metric used, even though some variables are more sensitive to the forcing than others (Figure 4). The largest expansion is seen in OLR ( $0.95^\circ$ ), followed by the Hadley cell edge ( $0.83^\circ$ ), and with P minus E giving the smallest widening ( $0.58^\circ$ ). Such differences in the trends simply represent a manifestation of the differing physics represented by the different metrics [Davis and Rosenlof, 2012; Lucas *et al.*, 2014; Solomon *et al.*, 2016]. For example, OLR is related to the temperature distribution and consequently represents the zonal mean

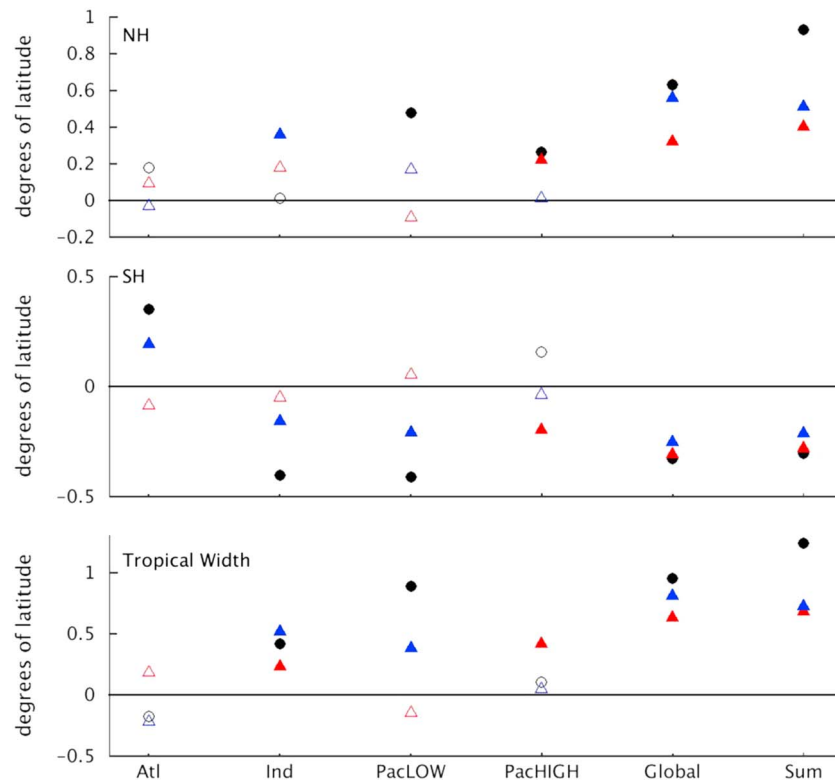


**Figure 4.** Tropical widening from the idealized experiments as given by OLR (black), Hadley cell (blue), and P-E (red). The last column represents the tropical widening as a sum of the first four idealized experiments. For the SH, negative (positive) means poleward expansion (equatorward contraction). The solid markers represent values that are significant at 95% significance level.

circulation (following from the geostrophic balance in the zonal-mean meridional momentum equation), in contrast with others, like the zonal mean meridional circulation, which is ageostrophic and connected to the eddy momentum fluxes and the zonal wind at the surface [Davis and Birner, 2017].

Further, our idealized experiments show that each basin is responsible for a different expansion rate; however, the sum of the trends does add up (very well in the SH and less well in the NH) closely to the expansion driven by the global SST trends. This implies that the processes involved in tropical widening depend quasi-linearly on the SST forcing, with nonlinearities accounting for the difference between the two solutions. Nonetheless, it gives confidence in the separation of the tropical widening into processes that are associated with distinct ocean sectors. This also suggests that some cancelation does take place; i.e., an expansion forced by SSTs in one basin may partly cancel out with a contraction forced by SSTs from another basin. One good example is that the SH poleward shift of the subtropics seen in OLR and forced by SSTs in the Tropical Pacific and Indian Ocean is partly cancelled out by a contraction that is forced by the SSTs in the high-latitude Pacific and the Atlantic.

The forcing in the Tropical Pacific results in an expansion in both hemispheres, bigger for OLR and smaller for the Hadley cell. In contrast, based on P-E, the subtropics experience a small contraction in both hemispheres. It is interesting to note the symmetry of the response among the metrics between the Northern and the Southern Hemisphere, which is not the case when the other idealized experiments are considered. Another interesting point is the wide range of tropical widening for this experiment, ranging from  $-0.1$  to  $0.9^\circ$ . This could be due to the fact that the position of the subtropics is outside of the forcing area, which stretches from  $25^\circ\text{S}$  to  $25^\circ\text{N}$ , and that different variables have a different sensitivity to remote SST forcing. The forcing in the midlatitude Pacific, which has some degree of symmetric with respect to the equator, is associated with a symmetric response in the two hemispheres as seen from P-E (expansion) and MMC (almost no response). However, when we look at OLR, the NH experiences an expansion and the SH exhibits a contraction, which implies that differences in the SST forcing and the land-ocean contrast between the

two hemispheres play an important role. Also, despite the fact that the SST anomalies in the Pacific dominate in size and magnitude, our results show that the Indian Ocean also contributes to the widening of the tropics in both hemispheres. Note that the SST anomalies in the Indian Ocean during 1993–2012 have the opposite sign compared to the anomalies from the SST pattern associated with the maximum expansion in the CMIP5 control runs (Figure 2). This implies that the expansion attributed to the warming of the Indian Ocean is rather independent from what is happening in the Pacific Ocean. Unlike the other basins, the Atlantic seems to have a more modest effect on the tropical width, with an average expansion, among metrics, close to zero.

#### 4. Discussion and Conclusions

Our study shows that the expansion of the tropics has a significant component that is associated with natural variability. Unforced simulations with a number of models from the CMIP5 data set are capable of reproducing a widening of the tropics that is comparable and even exceeds the one seen in observations, at least when measured via outgoing radiation fields as observed by satellites. By this measure, the ability of models to simulate as much widening of the tropics as observed is determined by the model's internal variability; i.e., models with bigger internal variability exhibit a larger tropical widening, and models that underestimate it fail to do so. On the other hand, when tropical expansion is measured via streamfunction or P-E, reanalysis fields imply much more expansion than OLR.

We find that, at least in models, the three width measures examined largely capture the same phenomenon, in contrast to the picture emerging from *Davis and Birner* [2017] and *Solomon et al.* [2016] based on other metrics. First, our three metrics are well correlated; second, regardless of metric, the expansion periods are associated with similar SST and OLR patterns, which resemble the IPO/PDO; and third, peak widening rates are similar in all metrics in models, though not in observations. Regarding those, the maximum trend in either of the reanalysis-based measures varies widely depending on the reanalysis. Therefore, we suspect that these are unreliable due to inhomogeneity of the reanalyses (which is expected from temporal inhomogeneity of available data, especially satellite sounding data). It is, however, also possible that real-world tropical width variations are more complex than those in models.

Idealized experiments with an atmospheric model forced with global and regional SSTs show that the maximum tropical widening observed during 1993–2012 is mostly associated with low-frequency changes in SSTs from the Tropical Pacific and the Indian Ocean, mirroring recent findings for decadal variations in global mean warming [*Zhou et al.*, 2016].

Our results imply that much of the observed tropical expansion simply reflects natural decadal variability, driven by SSTs, in agreement with other recent findings [*Allen and Ajoku*, 2016; *Allen et al.*, 2014; *Adam et al.*, 2014; *Quan et al.*, 2014; *Lucas and Nguyen*, 2015]. This finding greatly mitigates the uncertainty around tropical expansion that has prevailed since its discovery, especially around the magnitude and its causes. If the recent trend in SSTs is part of a natural fluctuation, then longer-term expansion of the tropics is likely to be significantly less than in recent decades. Moreover, 21st century model projections suggest that recovery of the stratospheric ozone concentrations will likely counter the southern-hemisphere tropical expansion driven by increased GHGs [*Son et al.*, 2009; *Allen and Ajoku*, 2016].

#### Acknowledgments

This work is funded by a Laureate Fellowship from the Australian Research Council. The computations were carried out with high-performance computing support provided by the National Computing Infrastructure (NCI) in Canberra, Australia. The data produced for and analysed in this paper are archived at NCI and can be provided upon request.

#### References

- Adam, O., T. Schneider, and N. Harnik (2014), Role of changes in mean temperature gradients in the recent widening of the Hadley circulation, *J. Clim.*, *27*, 7450–7461.
- Allen, R. J., and O. Ajoku (2016), Future aerosol reductions and widening of the northern tropical belt, *J. Geophys. Res. Atmos.*, *121*, 6765–6786, doi:10.1002/2016JD024803.
- Allen, R. J., S. C. Sherwood, J. R. Norris, and C. S. Zender (2012), Recent Northern Hemisphere tropical expansion primarily driven by black carbon and tropospheric ozone, *Nature*, *485*, 350–354.
- Allen, R. J., J. R. Norris, and M. Kovilakan (2014), Influence of anthropogenic aerosols and the Pacific Decadal Oscillation on tropical belt width, *Nat. Geosci.*, *7*, 270–274.
- Davis, N., and T. Birner (2017), On the discrepancies in tropical belt expansion between reanalyses and climate models and among tropical belt width metrics, *J. Clim.*, doi:10.1175/JCLI-D-16-0371.1.
- Davis, S. M., and K. H. Rosenlof (2012), A multidagnostic intercomparison of tropical width time series using reanalysis and satellite observations, *J. Clim.*, *25*, 1061–1078.
- Dee, D. P., et al. (2011), The ERA-Interim reanalysis: Configuration and performance of the data assimilation system, *Q. J. R. Meteorol. Soc.*, *137*, 553–597.
- Emile-Geay, J., R. Seager, M. A. Cane, E. R. Cook, and G. H. Haug (2007), Volcanoes and ENSO over the past millennium, *J. Clim.*, *21*, 3134–3148.
- Grassi, B., G. Redaelli, P. O. Canziani, and G. Visconti (2012), Effects of the PDO phase on the tropical belt width, *J. Clim.*, *25*, 3282–3290.

- Hartman, D. L., et al. (2013), Observations: Atmosphere and surface, in *Climate Change 2013: The Physical Science Basis. Contribution of Working Group I to the Fifth Assessment Report of the Intergovernmental Panel on Climate Change*, Cambridge Univ. Press, Cambridge, U. K., and New York.
- Hu, Y., and Q. Fu (2007), Observed poleward expansion of the Hadley circulation since 1979, *Atmos. Chem. Phys.*, *7*, 5229–5236.
- Hu, Y., L. Tao, and J. Liu (2013), Poleward expansion of the Hadley circulation in CMIP5 simulations, *Adv. Atmos. Sci.*, *30*, 790–795.
- Jackson, D. L., D. P. Wylie, and J. J. Bates (2003), The HIRS pathfinder radiance data set (1979–2001), paper presented at 12th Conference on Satellite Meteorology and Oceanography, Long Beach, Calif.
- Johanson, C. M., and Q. Fu (2009), Hadley cell widening: Model simulations versus observations, *J. Clim.*, *22*, 2713–2725.
- Kalnay, E., et al. (1996), The NCEP/NCAR 40-years reanalysis project, *Bull. Am. Meteorol. Soc.*, *77*, 437–471.
- Kanamitsu, M., W. Ebisuzaki, J. Woollen, S.-K. Yang, J. J. Hnilo, M. Fiorino, and G. L. Potter (2002), NCEP-DOE AMIP-II Reanalysis, (R-2), *Bull. Am. Meteorol. Soc.*, *83*, 1631–1643.
- Kang, S. M., L. M. Polvani, J. C. Fyfe, and M. Sigmond (2012), Impact of polar ozone depletion on subtropical precipitation, *Science*, *332*, 951–954.
- Kobayashi, S., et al. (2015), The JRA-55 reanalysis: General specifications and basic characteristics, *J. Meteorol. Soc. Japan*, *93*, 5–48.
- Kovilakam, M., and S. Mahajan (2015), Black carbon aerosol-induced Northern Hemisphere tropical expansion, *Geophys. Res. Lett.*, *42*, 4964–4972, doi:10.1002/2015GL064559.
- Lee, H.-T., A. Gruber, R. G. Ellingson, and I. Laszlo (2007), Development of the HIRS outgoing longwave radiation climate dataset, *J. Atmos. Oceanic Technol.*, *24*, 2029–2047.
- Lu, J., G. A. Vecchi, and T. Reichler (2007), Expansion of the Hadley cell under global warming, *Geophys. Res. Lett.*, *34*, L06805, doi:10.1029/2006GL028443.
- Lu, J., G. Chen, and D. M. W. Frierson (2008), Response of the zonal mean atmospheric circulation to El Niño versus global warming, *J. Clim.*, *21*, 5835–5851.
- Lu, J., C. Deser, and T. Reichler (2009), Cause of the widening of the tropical belt since 1958, *Geophys. Res. Lett.*, *38*, L03803, doi:10.1029/2008GL036076.
- Lucas, C., and H. Nguyen (2015), Regional characteristics of tropical expansion and the role of climate variability, *J. Geophys. Res. Atmos.*, *120*, 6809–6824, doi:10.1002/2015JD023130.
- Lucas, C., H. Nguyen, and B. Timbal (2012), An observational analysis of Southern Hemisphere tropical expansion, *J. Geophys. Res.*, *117*, D17112, doi:10.1029/2011JD017033.
- Lucas, C., B. Timbal, and H. Nguyen (2014), The expanding tropics: A critical assessment of the observational and modelling studies, *WIREs Clim. Change*, *5*, 89–112, doi:10.1002/wcc.251.
- McLandress, C., T. G. Shepherd, J. F. Scinocca, D. A. Plummer, M. Sigmond, A. I. Jonsson, and M. C. Reader (2011), Separating the dynamical effects of climate change and ozone depletion. Part II: Southern Hemisphere troposphere, *J. Clim.*, *24*, 1850–1868.
- Newman, M., et al. (2016), The Pacific Decadal Oscillation, revisited, *J. Clim.*, doi:10.1175/JCLI-D-15-0508.1.
- Nguyen, H., C. Lucas, B. Timbal, and L. Hanson (2015), Expansion of the Southern Hemisphere Hadley cell in response to greenhouse gas forcing, *J. Clim.*, *28*, 8067–8077.
- Polvani, L. M., D. W. Waugh, G. J. P. Correa, and S.-W. Son (2011), Stratospheric ozone depletion: The main driver of twentieth-century atmospheric circulation change in the Southern Hemisphere, *J. Clim.*, *24*, 795–812.
- Quan, X.-W., M. P. Hoerling, J. Perlwitz, H. F. Diaz, and T. Xu (2014), How fast are the tropics expanding, *J. Clim.*, *27*, 1999–2013.
- Seidel, D. J., Q. Fu, W. J. Randel, and T. J. Reichler (2008), Widening of the tropical belt in a changing climate, *Nat. Geosci.*, *1*, 21–24.
- Sherwood, S. C. (1996), Maintenance of the free-tropospheric tropical water vapour distribution, part II: Simulation by large-scale advection, *J. Clim.*, *9*, 2919–2934.
- Shi, L., and J. J. Bates (2011), Three decades of intersatellite-calibrated High-Resolution Infrared Radiation Sounder upper tropospheric water vapour, *J. Geophys. Res.*, *116*, D04108, doi:10.1029/2010JD014847.
- Solomon, A., L. M. Polvani, D. W. Waugh, and S. M. Davis (2016), Contrasting upper and lower atmospheric metrics of tropical expansion in the Southern Hemisphere, *Geophys. Res. Lett.*, *43*, 10,496–10,503, doi:10.1002/2016GL070917.
- Son, S.-W., N. F. Tandon, L. M. Polvani, and D. W. Waugh (2009), Ozone hole and Southern Hemisphere climate change, *Geophys. Res. Lett.*, *36*, L15705, doi:10.1029/2009GL038671.
- Son, S.-W., et al. (2010), Impact of stratospheric ozone on Southern Hemisphere circulation change: A multimodel assessment, *J. Geophys. Res.*, *115*, D00M07, doi:10.1029/2010JD014271.
- Waugh, D. W., C. I. Garfinkel, and L. M. Polvani (2015), Drivers of the recent tropical expansion in the Southern Hemisphere: Changing SSTs or ozone depletion?, *J. Clim.*, *28*, 6581–6586.
- Zhou, C., M. D. Zelinka, and S. A. Klein (2016), Impact of decadal cloud variations on the Earth's energy budget, *Nat. Geosci.*, *9*, 871–875.